Experimental Observation of Suppression of Coherent-Synchrotron-Radiation–Induced Beam-Energy Spread with Shielding Plates

V. Yakimenko, M. Fedurin, V. Litvinenko, A. Fedotov, D. Kayran, and P. Muggli

EXPERIMENTAL OBSERVATION OF SUPPRESSING CSR-INDUCED BEAM ENERGY SPREAD WITH SHIELDING PLATES

V. Yakimenko[1], M. Fedurin[1], V. Litvinenko[1,2], A. Fedotov[1], D. Kayran[1], P. Muggli[3]

[1] *Brookhaven National Laboratory, 820, Upton, NY 11973, USA*
[2] *Department of Physics and Astronomy, Stony Brook University, NY 11974, USA*
[3] *Max-Planck-Institut für Physik, Föhringer Ring 6, 80805 München, Germany*

We describe the first direct observation of the significant suppression of the energy spread induced by coherent synchrotron radiation (CSR) by a pair of conductive plates placed inside a dipole magnet. In addition to various feedback loops improving the energy stability of the beam parameters, our key innovation for this experiment is the observation of the time-resolved energy-variation within the electron bunch, instead of the traditionally measured RMS energy spread. We present the results of the experiments and compare them with a rigorous analytical theory.

There are many publications on coherent synchrotron radiation or CSR wakefields and their effect on bunch quality; a comprehensive review of this topic can be found in [1]. With the advent of high-brightness beams and the increase number of their applications, for example to advanced light sources such as the LCLS, the minimization or suppression of the detrimental effects of CSR on short particle bunches quality is an important and timely issue. Methods proposed to address that issue include bunch lengthening and the addition of RF cavities operating at higher harmonics to "flatten" the RF curvature and thus decrease the energy spread. Such methods are complex and costly while using parallel conducting plates is a much simpler, cost-effective solution that has important consequences in beam line design.

The possibility of using shielding plates to minimize CSR wakes was suggested more than half a century ago [2]. The suppression of the beam-average value of the CSR-induced energy loss in such scheme was demonstrated experimentally [3]; the measurements agreed well with theoretical predictions [4]. The authors of recent theoretical studies [5] concluded that, while shielding plates can eliminate CSR-induced average energy loss, CSR-induced correlated energy-spread remains. Our experimental observations and supporting theoretical estimates discussed in this Letter lead to a different conclusion: the shielding plates can also greatly reduce the energy spread induced by CSR-wakes in a bending magnet. To our knowledge, this is the first experimental demonstration of such a suppression effect.

The experiment was carried out at the Brookhaven Accelerator Test Facility. We estimated that with our beam parameters and, for a single pass through the dipole magnet, the CSR-induced energy change to the bunch spectrum is at the level of tens of keVs. Consequently, we needed a beam energy-stability $\delta E/E$ of $\sim 10^{-5}$ to reliably characterize this effect. The high-brightness electron beam was produced by a 1.6 cell photoinjector RF gun, and then accelerated by a 6m long S-band linac to 57.6MeV. The beam geometric emittance is $\sim$17nm-rad. Acceleration off the crest of the RF wave induced linear energy-time correlation (chirp) along the beam. In the dispersive region of the transport line, after a first dipole magnet we employed an energy-selection collimator (or slit) to produce a 2ps-long bunch by allowing a 200keV-wide slice of the original chirped beam to pass through. As a result, we created very stable beam conditions at the dipole magnet: a slightly different part of the original beam was selected in time due to a natural shot-to-shot energy jitter, yet the selected beam had the same energy spectrum. We also used a slow feedback system that stabilized the relative beam energy variations below the 10^{-4} level, and the RF phase at the quarter degree (approximately 250 femtoseconds) level.

This selection/stabilization method is very similar to the mask technique that was developed and actively used for different experiments at ATF, and is detailed in [6]. A large ratio of horizontal dispersion to beta functions at the location of the energy collimator ($s\sim$12.5 m in Fig. 1), along with low emittance and low local- energy-spread allowed for the generation of a flat-top bunch current with sharp rise and fall time of $\sim$200fs. We used the linear energy-time correlation of the selected bunch to measure the beam's length by analyzing beam images on the energy spectrometer. Aluminum shielding plates were installed in the second dipole (s=20m in Fig. 1)magnet where CSR effects are much stronger than it the first one since the bunch is shorter and has sharp edges. The material was polished to a submicron level of flatness to reduce the influence of wakefields associated with surface roughness. The dipole magnet is 0.4-meter long, with a 20-degree bending angle. The plates extended 0.15 m on each side of the dipole to cover the edge-field regions for a total plate- length of 0.7 m. We could change their vertical distance from the beam axis with sub-millimeter accuracy.
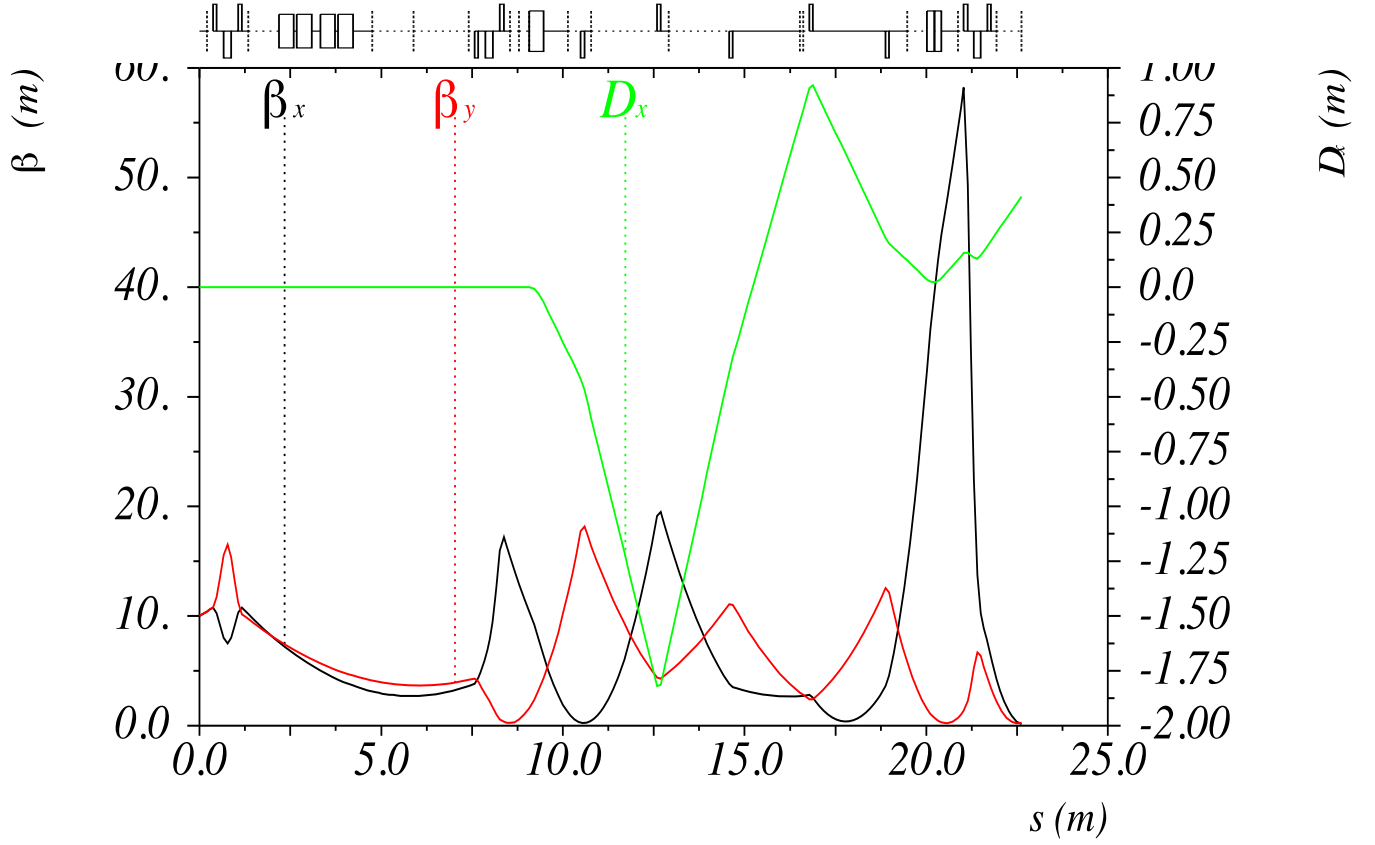
Figure 1: Beam's optical function along the transport line from the linac exit to the spectrometer-beam profile monitor. The beta functions are defined as $\beta_{x,y}=\sigma_{x,y}/\varepsilon$, where $\sigma_{x,y}$ are the beam transverse sizes in the x and y planes, respectively, and ε is the beam geometrical emittance. The dispersion is labeled as D (green line). The energy collimator is located at position s=12.5m, and the magnet with shielding plates at s=20m. The energy spectra were measured on a screen at s=22.5m.

Fig. 1 illustrates the beam optical functions starting from the linac exit and to the energy spectrometer. Focusing was designed to have a zero dispersion function in the center of the magnet with the shielding plates (s=20m) so as to minimize the influence of transverse size effects. A small vertical beta-function combined with low emittance were essential to ensure the 100% beam transmission through the 0.7-m-long shielding plates when they were closed to a minimum gap of 1mm. The large number of beam profile monitors available along the transport line allowed for experimentally verifying the optical functions depicted in Fig. 1 to better than 10% accuracy.

The beam duration was measured via autocorrelation of the coherent-transition radiation (CTR) generated by the beam when entering a copper mirror. The trace in Fig. 2 was measured with a Michelson interferometer in combination with

a liquid-helium-cooled bolometer. Low- and high- frequency cut-offs of the measurement system were accounted for in our analysis; we concluded that the bunch had a 600 μm-long flat top with rise and fall lengths of 60 um (or 200 fs); these values agree well with estimates of bunch length based on the optical functions at the collimator [6].
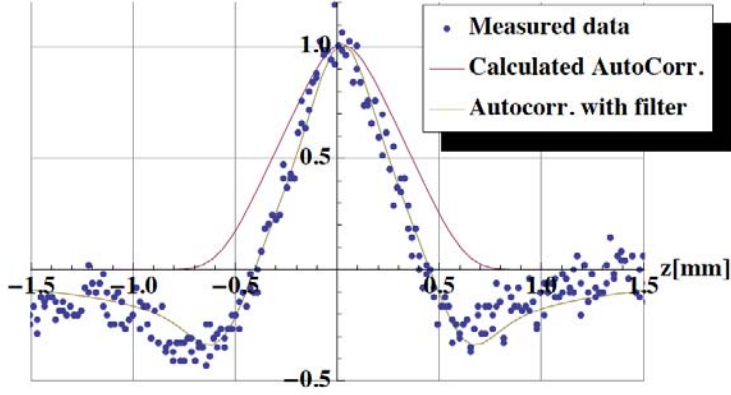

Figure 2: Measured CTR autocorrelation trace of the electron beam (points). The violet line is the calculated auto-correlation trace for a 600 μm-long flat-top bunch with 60 micron rise/fall lengths. The brown line is the calculated auto-correlation trace taking into account the low- and high-frequency cut-offs of the measurement system; it reproduces the measured trace.

As Fig.1 shows, the beam was focused tightly on the beam-profile monitor (s=22.5m) by the quadrupole triplet following the second dipole. Accordingly, we obtained high-resolution energy spectra by summing the images along the non-dispersed direction. Fig. 3 is a composite of the energy spectra for different plate gaps The minimum gap is 1mm.
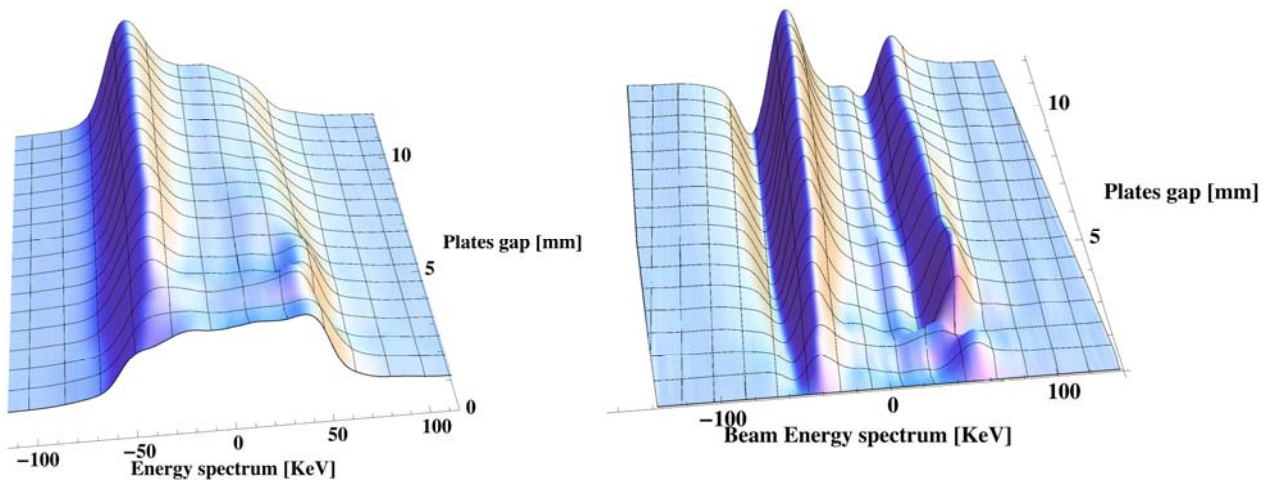
Figure 3: Measured beam-energy spectra as function of the gap between the shielding plates (on the left). Charge displacement map calculated from this result by subtracting the energy spectrum obtained with the plate gap of 1mm from the other spectra is shown on the right.

In this case, we selected the energy correlation imposed on the incoming beam such that the head of the beam had a lower energy than its tail. Fig. 3 clearly shows that for larger plate openings, particles in the head of the beam (lowest energy) gain energy, and move towards the middle of the energy distribution. Similarly particles in the tail (highest energy) lose energy, and also move toward the middle of the distribution. This energy exchange is not observable at small gaps, between $\sim$ 1 and 3 mm. Therefore, at small gap values the CSR-induced bunch energy spread is suppressed by the plates. This effect is even more apparent in Fig. 3 (right) where we plot the difference between the energy spectra for various plate openings and that for the minimum opening of $\sim$1mm.

The simple geometry of two parallel conducting plates allows for the derivation of an exact analytical expression for the CSR wakefields for an arbitrary longitudinal-bunch profile. We start with classical expressions for the retarded radiated field for a single electron [7]:

$$\vec{E}(\vec{r_t},t) = \left\{ e\frac{1-\beta^2}{\left(1-\vec{\beta}\vec{R}\right)^3}\left(\vec{R}-\vec{\beta}R\right) + \frac{e}{c\left(R-\vec{\beta}\vec{R}\right)^3}\left[\vec{R}\times\left[\left(\vec{R}-\vec{\beta}R\right)\times\dot{\vec{\beta}}\right]\right] \right\}_{ct'=t+R} \tag{1}$$

The first term in the right hand side of eq. (1) is the well-known static term while the second term corresponds to the radiation field.

We consider a radiating electron moving along circular orbit with a constant speed, $\vec{\beta}=\vec{v}/c$, a constant radius R_0 and $\omega = c\beta/R_0$. A test electron moves along the same trajectory but at a different time: $r = R_0, z = 0, \theta_t = \theta_1 + \omega t$.
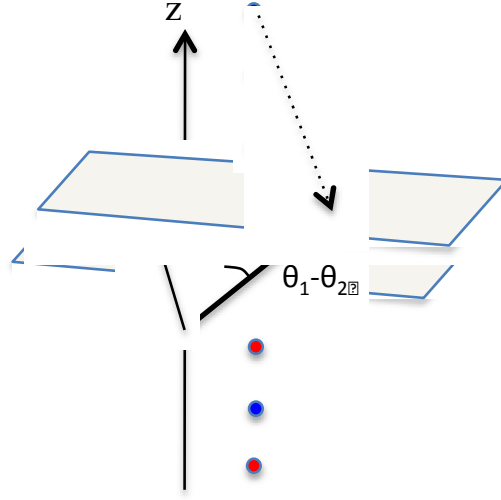
Figure 4. Two particles on the common bent trajectory of R_0 with two vertically displaced metal plates: the green is a test particle, and the red is a radiating one with its image charges of alternating sign. The dashed arrow shows the vector between the radiating charge and the test particle.

Two ideal conducting-plates are located at $z_p = \pm h/2$. The charge-distribution inside the plates is equivalent to that of a set of point charges located at the same $r = R_0, \theta_r = \theta_0 + \omega t$ but at $z = nh; n \in \{-\infty ... -1, 0, 1, 2..., \infty\}$. The sign of the charge is alternating as $q = (-1)^n e$. Because the interaction between particles does not depend on time, we use the relative variables:

$$\vec{r}_r(t') = R_0(\hat{x}\cos\theta_r + \hat{y}\sin\theta_r) \to \vec{r}_n(t') = R_0(\hat{x}\cos\theta_n + \hat{y}\sin\theta_n) + \hat{z}nh \quad \text{and} \quad \vec{r}_t(t) = R_0(\hat{x}\cos\theta_t + \hat{y}\sin\theta_t) \quad \text{with}$$

$$\vec{R} = \vec{r}_t(t) - \vec{r}_n(t') = -2R_0\sin\psi(\hat{x}\sin\phi + \hat{y}\cos\phi) - \hat{z}nh \quad . \quad \text{Here} \quad \psi = \frac{\theta_t(t) - \theta_t(t')}{2} \quad \text{and} \quad \varphi = \frac{\theta_t(t) + \theta_n(t')}{2} \quad \text{are}$$

parameterizations for $\theta_t(t)$ at the retarded time t' [8].

The expression for the total longitudinal CSR wake-field can be written as

$$W(\varphi) = \frac{2e\beta^2}{R_o^2} N_e \sum_{n=-\infty}^{\infty} (-1)^n \int_{-\infty}^{\infty} d\psi \cdot f(\varphi - 2\psi + \beta\rho_n(\psi)) \cdot \left(1 - \beta\frac{\sin 2\psi}{\rho_n(\psi)}\right) \cdot$$

$$\frac{\left(-\rho_n^2(\psi)\sin 2\psi + 2\sin^2\psi\rho_n(\psi)\beta + 4\cos\psi\sin^3\psi\right)}{\left(\rho_n(\psi) - \beta\sin 2\psi\right)^3}$$

(2)

where $f(\varphi)$ is the normalized beam charge distribution, and R_o is the radius of curvature of the electron's trajectory in the bending magnet. The expression $\rho_n(\psi) = \sqrt{4\sin^2\psi + n^2 h^2 / R_o^2}$ in eq. (2) is nothing else than the dimensionless distance between the radiation and the observation point.

In this short letter, we show only few selected results. First, Fig. 5 illustrates the calculated CSR wakefields using the analytical formula (2), and the electron beam profile described in Fig. 2.
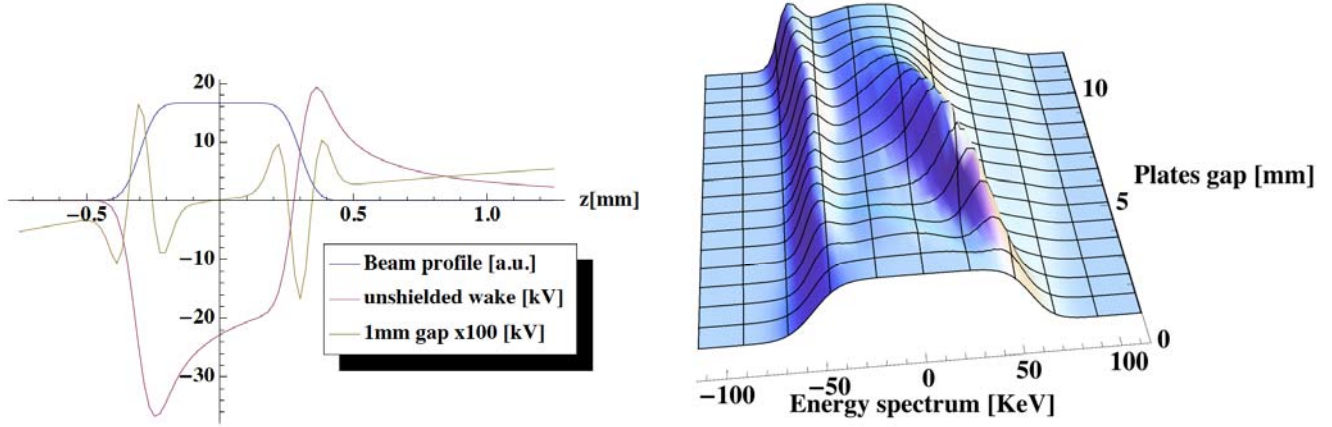

Figure 5: Calculated CSR wakefields for the unshielded- and shielded-case with 1mm plates gap from Eq. 2 (on the left). For clarity the CSR wakefield for the 1mm gap is magnified a hundred-fold. Simulated dependence of the beam energy spectrum on the gap between the plates is plotted on the right. The similarity of the features herein to the experimental observations depicted in Fig. 3 verifies the excellent agreement of the experimental- and theoretical- findings.

The value of the wakefield sampled by the beam itself is of greatest practical importance since it affects both the average energy loss and the energy spread. We call the variation in the wakefield experienced by the electron beam its span. It is clear from these direct calculations that a small gap reduces both the CSR-induced energy loss and spread. To be exact, closing the gap from 12 mm to 1mm reduces the span of CSR wakefield affecting the beam with decreases from 36 keV to 180 eV, i.e., a 200-fold reduction.

The results from our analytical studies demonstrate good qualitative agreement with the measurements. For example, both the exact analytical theory and the experiments show that only at very small gaps of ~ 1mm is there an effective suppression of the CSR wakefield span. Widening the gap from 1 mm to 2mm, increases the CSR wakefield span fourfold. With a 4mm gap, the span is almost identical to that of unshielded wake, even though it has more oscillations (i.e., less net loss) than the unshielded wake. It also is quite clear that plates with 12mm gap affect only the long-range wings of the wakefield, viz., they scarcely change the CSR effect on the beam.
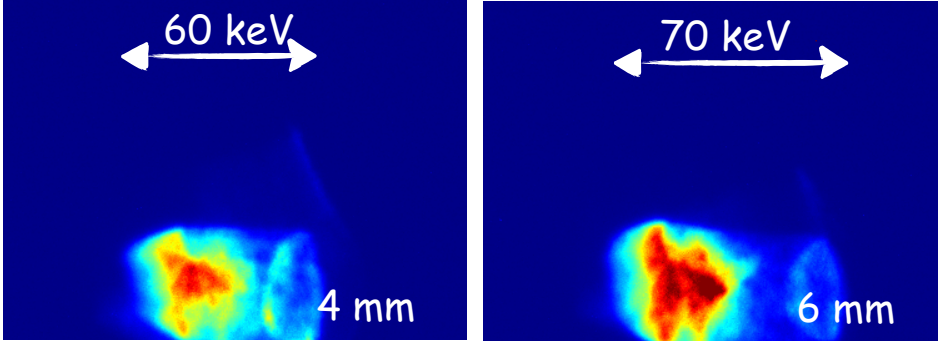
Figure 6: Spectrometer images that clearly demonstrate effect of CSR wake on a Gaussian beam for 4 and 6mm gaps. Beam energy distribution is spread along horizontal axis and vertical axis simply shows vertical beam profile at the spectrometer location.

In addition to demonstrating the suppression of the CSR-induced energy spread, we also observed the suppression of the CSR-induced average beam energy loss, similarly to previously observed in [3]. We used an approximately Gaussian beam of 0.3ps RMS duration, 10keV RMS energy spread and no correlated energy chirp. The resulting spectrometer images in Fig. 6 clearly demonstrate the effect of the CSR wake on this Gaussian beam for plates gaps of 4 and 6mm. The CSR wakefields calculated using Eq. 1 for that longitudinal beam-profile are presented in Fig. 7.
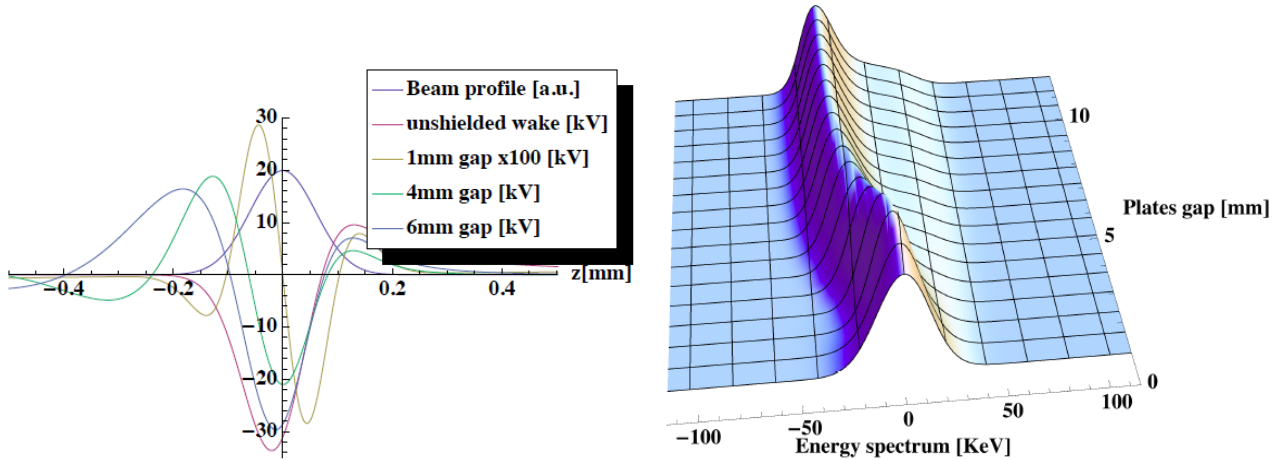

Figure 7: Calculated CSR wake for a Gaussian beam in free space and in the presence of shielding plates for various gaps is shown on the left. For visibility, the CSR wake-field for 1mm gap is multiplied by 100. Calculations of the beam energy spectrum dependence on the gap between the plates are shown on the right. The similarity of the figure to the

experimental observations of Fig. 6 demonstrates the excellent agreement between the experimental results and theoretical findings.

The typical 10^{-3}-10^{-4} level jitter for pulsed RF systems and inability to use slicing out part the chirped beam to further stabilize reference beam's energy did not allow for comparing the measured spectra for different plate gaps. The predictions from calculations are plotted in Fig. 7 and show excellent agreement with measured spectra profile shape.

ACKNOWLEDGMENTS

REFERENCES

[1] J. Murphy, ICFA Beam Dynamics Newsletter No. 35 (2004)

[2] L. I. Schiff, Rev. Sci. Instrum. 17, 6 (1946)

[3] R. Kato et.al, Phys. Rev. E 57, 3454–3460 (1998)

[4] J. S. Nodvick et.al, Phys. Rev. **96**, 180 (1954)

[5] C. Mayers and G. Hoffstaetter, PRST/AB 12, 024401 (2009)

[6] P. Muggli, et.al. Phys. Rev. Lett. **101**, 054801 (2008)

[7] L.D. Landau and E.M. Lifshitz, "The Classical Theory of Fields", Pergamon Press, Fourth Edition, 1975, p. 162, formula (63.8)

[8] V.N. Litvinenko, CSR, Duke FEL Lab Notes, 1998